



Thermal analysis of micro-channel heat exchangers with two-phase flow using FEM

Micro-channel heat exchangers

43

Accepted May 2004

Pradeep Hegde, K.N. Seetharamu, G.A. Quadir,

P.A. Aswathanarayana, M.Z. Abdullah and Z.A. Zainal

School of Mechanical Engineering, Universiti Sains Malaysia, Penang, Malaysia

Abstract

Purpose – To analyze two-phase flow in micro-channel heat exchangers used for high flux micro-electronics cooling and to obtain performance parameters such as thermal resistance, pressure drop, etc. Both uniform and non-uniform micro-channel base heat fluxes are considered.

Design/methodology/approach – Energy balance equations are developed for two-phase flow in micro-channels and are solved using the finite element method (FEM). A unique ten noded element is used for the channel discretization. The formulation also automatically takes care of single-phase flow in the micro-channel.

Findings – Micro-channel wall temperature distribution, thermal resistance and the pressure drop for various uniform micro-channel base heat fluxes are obtained, both for single- and two-phase flows in the micro-channel. Results are compared against data available in the literature. The wall temperature distribution for a particular case of non-uniform base heat flux is also obtained.

Research limitations/implications – The analysis is done for a single micro-channel and the effects of multiple or stacked channels are not considered. The analysis needs to be carried out for higher heat fluxes and the validity of the correlation needs to be ascertained through experimentation. Effects of flow mal-distribution in multiple channels, etc. need to be considered.

Practical implications – The role of two-phase flow in micro-channels for high flux micro-electronics cooling in reducing the thermal resistance is demonstrated. The formulation is very useful for the thermal design and management of microchannels with both single- and two-phase flows for either uniform or non-uniform base heat flux.

Originality/value – A simple approach to accurately determine the thermal resistance in micro-channels with two-phase flow, for both uniform and non-uniform base heat fluxes is the originality of the paper.

Keywords Finite element analysis, Flow, Thermal resistance, Pressure

Paper type Technical paper

Nomenclature

Bo = boiling number

C = Martinelli-Chisholm constant

C_p = specific heat at constant pressure, J/kg K

D_h = hydraulic diameter of micro-channel, m

e = liquid droplet quality

f = liquid film quality

f_f = friction factor based on local liquid flow rate

G = mass velocity, kg/m²s

H_c = height of the micro-channel, m

h_{tp} = saturated two-phase heat transfer coefficient, W/m²K

I = enthalpy, J/kg

I_L = saturation enthalpy of the coolant, J/kg

I_{fg} = latent heat of vaporization, J/kg

I_{tp} = enthalpy of the two-phase mixture, J/kg

k = thermal conductivity of the micro-channel material, W/m K

k_f = coolant thermal conductivity, W/m K

L = length of the micro-channel, m

L_e = length of the Finite element, m

\dot{m} = mass flow rate of the coolant, kg/s



N	= number of micro-channels in the heat sink	<i>Greek symbols</i>	
P	= pressure, bar	α	= aspect ratio = H_c/w_c
ΔP	= pressure drop, bar	δ	= liquid film thickness, m
q	= heat flux, W/cm^2	μ	= liquid viscosity, Ns/m^2
R	= thermal resistance, $^\circ C/W$	ρ	= density of the liquid, kg/m^3
Re	= Reynolds number	ε	= void fraction
T	= micro-channel wall temperature, $^\circ C$	ϕ_f	= two-phase friction multiplier
T_f	= coolant temperature, $^\circ C$	<i>Subscripts</i>	
T_{sat}	= saturation temperature of the coolant, $^\circ C$	a	= annular flow
t	= fin half thickness, m	f	= liquid phase
v	= specific volume, m^3/kg	g	= vapor phase
W	= width of the micro-channel heat sink, m	in	= inlet of the micro-channel
w_c	= width of a single micro-channel, m	out	= outlet of the micro-channel
X_{vv}	= Martinelli parameter based on laminar liquid- laminar vapor flow	sp	= single-phase flow
x	= vapor quality	tp	= two-phase flow
x_e	= thermodynamic equilibrium quality		

Introduction

Thermal management is a burning issue in the microelectronic industry in view of rapid miniaturization. Large heat fluxes of the order of $50-150 W/cm^2$ are not uncommon in the case of microprocessors. Tuckerman and Pease (1981) have demonstrated that, by utilizing the micro-channels etched on the back of chips as cooling passages the thermal resistance between the active die and the surrounding medium can be rendered very small. In view of the very small dimensions of micro-channel passages, the heat transfer coefficients will be very large and thus effective heat removal from the chips is possible. Sufficient data regarding forced convective single-phase flow in micro-channels are available in literature. Peng and Peterson (1996) investigated water flow in rectangular micro-channels with hydraulic diameters ranging from 0.133 to 0.367 mm. In laminar flows it was found that the heat transfer depends on the aspect ratio and the ratio of hydraulic diameter to the center to-center distance of the micro-channels. Zhimin and Fah (1997) analyzed the flow and heat transfer in micro-channels through a thermal resistance model assuming uniform distribution of heat load on the base of the heat sink. Kim and Kim (1999) reported analytical solutions for both velocity and temperature profiles in micro-channel heat sinks by modeling the micro-channel heat sink as a fluid-saturated porous medium. They gave an expression for the total thermal resistance which was derived from the analytical solutions and the geometry of the micro-channel heat sink for which the thermal resistance of the heat sink is minimal. Quadir *et al.* (2001) have analyzed single-phase flow in micro-channels by the finite element method (FEM), including the case of non-uniform heat flux from the chip. Toh *et al.* (2002) investigated three-dimensional fluid flow and heat transfer inside micro-channels by solving the steady laminar flow and heat transfer equations using the finite-volume method.

Although single-phase micro-channel heat sinks are capable of dissipating high heat fluxes, the small coolant flow rate produces a large temperature rise along the flow direction, thus considerably reducing the temperature driving potential ($T - T_f$) for convective heat transfer. As a result, the device efficiency reduces as the

coolant reaches the exit. In order to overcome the above said problem, the coolant may be allowed to boil inside the micro-channel. Boiling convection in micro-channels is promising because of the various advantages such as:

- two-phase flow in micro-channels results in higher heat transfer coefficient as compared to single-phase flow;
- two-phase flow results in constant fluid temperature ($T_f = T_{\text{sat}}$) in the stream-wise direction, thus not affecting the temperature driving potential ($T - T_f$); and
- flow rate and coolant inventory requirements are less.

In spite of the above-cited advantages, boiling flow in micro-channels has received little attention owing to the more complicated physics involved. Bergles and Dorrmer (1969) performed one of the earliest studies of flow boiling in small tubes. Wambsganss *et al.* (1993) have investigated flow boiling of refrigerant R113 in small circular tubes. More recently, Qu and Mudawar (2002, 2003a, 2004) have analyzed several aspects of fluid flow and boiling in two-phase micro-channel heat sinks namely, boiling incipience, pressure drop, heat transfer characteristics, critical heat flux, etc. Qu and Mudawar (2003b, c) developed a detailed two-phase flow model assuming annular flow to dominate in water cooled micro-channels. Their analysis was supported by detailed experimentation.

The present paper analyzes both single-phase as well as two-phase flows in rectangular cross section micro-channels using the FEM. The results are presented in the form of the channel wall temperature distribution and overall thermal resistance for various uniform heat fluxes ranging from 40 to 150 W/cm². The case of non-uniform heat flux at the base of the micro-channel is also considered in the present analysis.

Method of analysis

Figure 1 shows a typical structure of a micro-channel heat sink used for electronics cooling. FEM is used for the thermal analysis of the micro-channel heat sink. For the finite element analysis, the micro-channel is divided into a number of elements along the stream-wise direction, i.e. length direction, using a unique ten-noded element, depicting the channel cross-section. The finite element along with the nodes is shown in Figure 2. Conduction heat transfer is considered in two directions in both the vertical walls. The base of the channel receives heat from the source and the heat is transferred to the coolant by convection directly from the base and indirectly through sidewalls. A uniform heat load is assumed at the base of the substrate for initial analysis. Subsequently non-uniform flux is also considered. An assembly of elements in the length-wise direction will complete the full channel. The method of discretization is very general and is capable of extending either longitudinally or transversely, or in both directions.

Single-phase flow

In the present analysis it is assumed that the coolant enters the micro-channel in a sub-cooled condition and subsequently boils in the micro-channel. Quadir *et al.* (2001) have analyzed single-phase flow in micro-channel heat sinks of optimal dimensions given by Kim and Kim (1999) using the above-mentioned methodology. The thermal

Figure 1.
A typical micro-channel
heat sink used for
electronics cooling

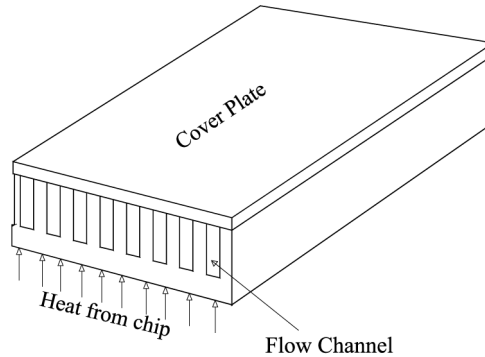
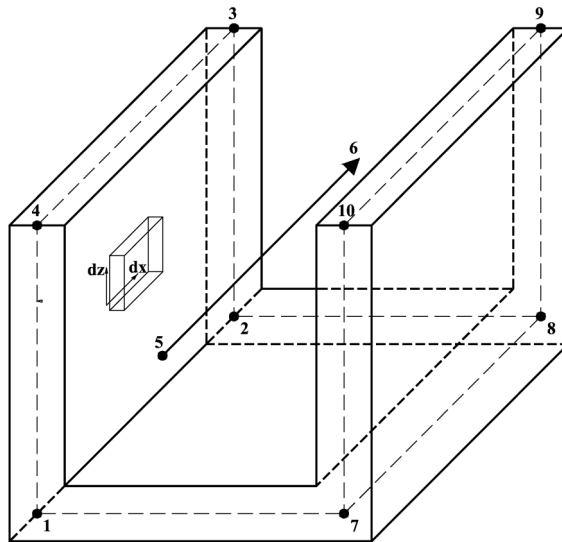


Figure 2.
Details of a single finite
element used for
discretization along with
its nodal points



resistances obtained by Quadir *et al.* (2001) match very well with that of Kim and Kim (1999) and also with that of Zhimin and Fah (1997). The same methodology is used for the analysis of single-phase section of the micro-channel and is further extended for the analysis of two-phase flow.

Two-phase flow

In two-phase flow region of the micro-channel the temperature of the fluid remains constant and is equal to the saturation temperature. However, the vapor quality goes on increasing as the coolant flows down the micro-channel. Care should be taken to see that the liquid does not get superheated or else the advantage of constant fluid temperature in the stream-wise direction is lost. The two-phase heat transfer coefficient is higher compared to that in single-phase flow but however, it does not remain constant and goes on varying in the stream-wise direction.

Governing equations

Considering the conduction and convection heat transfer, the following equation can be written for the left wall of the micro-channel:

$$k \frac{\partial^2 T}{\partial x^2} + k \frac{\partial^2 T}{\partial z^2} - \frac{h_{tp}}{t} (T - T_{sat})_{Left} = 0 \quad (1)$$

similarly for the right wall of the micro-channel the governing equation can be written as:

$$k \frac{\partial^2 T}{\partial x^2} + k \frac{\partial^2 T}{\partial z^2} - \frac{h_{tp}}{t} (T - T_{sat})_{Right} = 0 \quad (2)$$

The governing equation for the fluid, which receives heat from the two walls and the bottom surface, can be written as:

$$\dot{m} \frac{dI}{dx} - h_{tp} H_c (T - T_{sat})_{Left} - h_{tp} H_c (T - T_{sat})_{Right} - h_{tp} w_c (T - T_{sat})_{Bottom} = 0 \quad (3)$$

No separate equations need be written for the bottom wall, as equations (1)-(3) automatically take care of the nodes on the bottom wall as well. The governing equations and the subsequent formulations are very general in the sense that they can be applied to the single-phase flow region as well with minor modifications.

The temperature driving potential for the convective heat transfer ($T - T_{sat}$) is assumed to be the difference between average wall and the fluid saturation temperatures. Therefore,

$$(T - T_{sat})_{Left} = \left(\frac{1}{4} \sum_{i=1}^4 T_i \right) - T_{sat} \quad (4)$$

$$(T - T_{sat})_{Right} = \left(\frac{1}{4} \sum_{i=7}^{10} T_i \right) - T_{sat} \quad (5)$$

$$(T - T_{sat})_{Bottom} = \frac{1}{4} (T_1 + T_2 + T_7 + T_8) - T_{sat}$$

The micro-channel wall temperature is assumed to vary as:

$$T = \sum_{i=1}^4 N_i T_i \quad (6)$$

where, the shape function N_i for a general quadrilateral element is given by Segerlind (1984)

$$N_i = (1 + \xi \xi_i)(1 + \eta \eta_i) \quad (8)$$

where η_i, ξ_i are the local coordinates of the corner node i .

The coolant enthalpy is assumed to vary linearly as:

$$I = \sum_{j=5}^6 N_j I_j. \quad (9)$$

The shape functions for the linear element are given as (Segerlind, 1984):

$$N_1 = 1 - \frac{x}{L_e}, \quad N_2 = \frac{x}{L_e}.$$

Applying the Galerkin weighted residual integral to the governing equations, we write the complete set of equations as (Lewis *et al.*, 1996):

$$[K_e]\{T\} = \{f_e\}. \quad (10)$$

The element stiffness matrix can be written as:

$$[K_e] = \begin{bmatrix} K_{1-1} & K_{1-2} & K_{1-3} & K_{1-4} & K_{1-5} & K_{1-6} & 0 & 0 & 0 & 0 \\ K_{2-1} & K_{2-2} & K_{2-3} & K_{2-4} & K_{2-5} & K_{2-6} & 0 & 0 & 0 & 0 \\ K_{3-1} & K_{3-2} & K_{3-3} & K_{3-4} & K_{3-5} & K_{3-6} & 0 & 0 & 0 & 0 \\ K_{4-1} & K_{4-2} & K_{4-3} & K_{4-4} & K_{4-5} & K_{4-6} & 0 & 0 & 0 & 0 \\ K_{5-1} & K_{5-2} & K_{5-3} & K_{5-4} & K_{5-5} & K_{5-6} & K_{5-7} & K_{5-8} & K_{5-9} & K_{5-10} \\ K_{6-1} & K_{6-2} & K_{6-3} & K_{6-4} & K_{6-5} & K_{6-6} & K_{6-7} & K_{6-8} & K_{6-9} & K_{6-10} \\ 0 & 0 & 0 & 0 & K_{7-5} & K_{7-6} & K_{7-7} & K_{7-8} & K_{7-9} & K_{7-10} \\ 0 & 0 & 0 & 0 & K_{8-5} & K_{8-6} & K_{8-7} & K_{8-8} & K_{8-9} & K_{8-10} \\ 0 & 0 & 0 & 0 & K_{9-5} & K_{9-6} & K_{9-7} & K_{9-8} & K_{9-9} & K_{9-10} \\ 0 & 0 & 0 & 0 & K_{10-5} & K_{10-6} & K_{10-7} & K_{10-8} & K_{10-9} & K_{10-10} \end{bmatrix}.$$

where

$$\begin{aligned} K_{1-1} &= K_{2-2} = K_{3-3} = K_{4-4} = K_{7-7} = K_{8-8} = K_{9-9} = K_{10-10} = 2e_x + 2e_z + c \\ K_{1-2} &= K_{2-1} = K_{3-4} = K_{4-3} = K_{7-8} = K_{8-7} = K_{9-10} = K_{10-9} = -2e_x + e_z + c \\ K_{1-3} &= K_{2-4} = K_{3-1} = K_{4-2} = K_{7-9} = K_{8-10} = K_{9-7} = K_{10-8} = -e_x + e_z + c \\ K_{1-4} &= K_{2-3} = K_{3-2} = K_{4-1} = K_{7-10} = K_{8-9} = K_{9-8} = K_{10-7} = e_x - 2e_z + c \\ K_{1-5} &= K_{1-6} = K_{2-5} = K_{2-6} = K_{3-5} = K_{3-6} = K_{4-5} = K_{4-6} = K_{7-5} = K_{7-6} = K_{8-5} \\ &= K_{8-6} = K_{9-5} = K_{9-6} = K_{10-5} = K_{10-6} = -2c \\ K_{5-1} &= K_{5-2} = K_{6-1} = K_{6-2} = U + W1; \quad K_{5-3} = K_{5-4} = K_{6-3} = K_{6-4} = U \\ K_{5-5} &= K_{5-6} = -f_m - 2(U + V + W1); \quad K_{6-5} = K_{6-6} = f_m - 2(U + V + W1); \\ K_{5-7} &= K_{5-8} = K_{6-7} = K_{6-8} = V + W1 \quad K_{5-9} = K_{5-10} = K_{6-9} = K_{6-10} = V \\ c &= h_{tp}L_eH_c/16; \quad e_x = tkH_c/6L_e; \quad e_z = tkL_e/6H_c; \quad f_m = \dot{m}/2 \\ U &= -h_{tp}L_eH_c/8; \quad V = -h_{tp}H_cL_e/8; \quad W1 = -h_{tp}w_cL_e/8 \end{aligned}$$

The force vector and the temperature vector which includes the coolant enthalpies as well, are written as:

$$\{f_e\} = \frac{qA_b}{4} [1 \ 1 \ 0 \ 0 \ 0 \ 0 \ 1 \ 1 \ 0 \ 0]^T$$

where A_b is the micro-channel pitch \times Channel length and

$$\{T\} = [T_1 \ T_2 \ T_3 \ T_4 \ I_5 \ I_6 \ T_7 \ T_8 \ T_9 \ T_{10}]^T$$

where, $T_1, T_2, T_3, T_4, T_7, T_8, T_9$ and T_{10} are the micro-channel wall temperatures at the respective nodes, while I_5 and I_6 are coolant enthalpies at nodes 5 and 6, respectively.

The global stiffness matrix is obtained by assembling the element stiffness matrices in the stream-wise direction as explained in Segerlind (1984). A typical assembly of eight elements having 45 nodes is shown in Figure 3. For converging results the section of the micro-channel experiencing two-phase flow is discretized into 400 elements, owing to the greater flow complexities involved in two-phase flow, whereas the single-phase section of the micro-channel is discretized into 50 elements only.

Determination of the location of the onset of two-phase flow

The length of the micro-channel, experiencing single-phase flow L_{sp} and that experiencing two-phase flow L_{tp} can be calculated by heat balance and are given as:

$$L_{sp} = \frac{\dot{m}(I_{sat,0} - I_{in})}{qW} \tag{11}$$

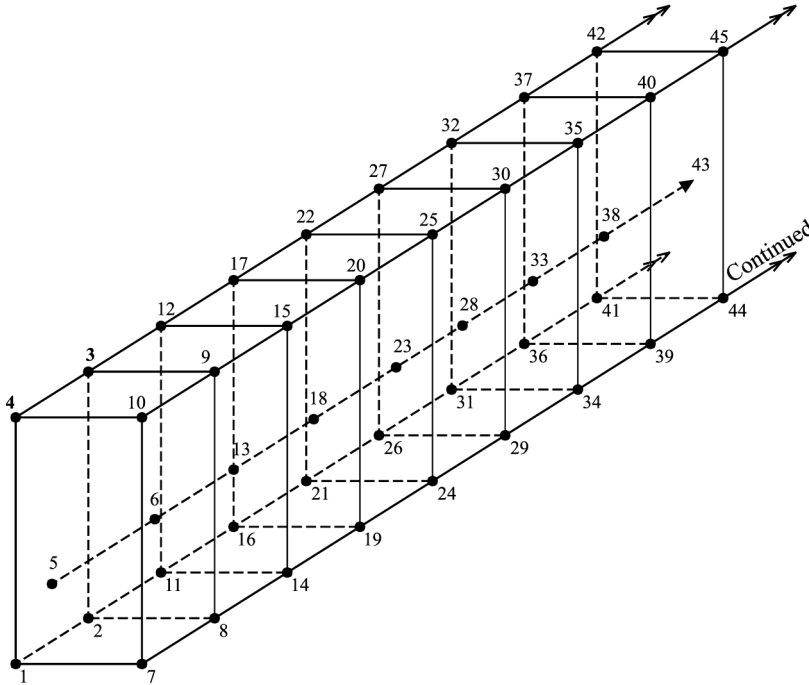


Figure 3.
A typical assembly of
eight finite elements in
the stream-wise direction

$$L_{tp} = L - L_{sp} \quad (12)$$

where $I_{sat,0}$ is the coolant enthalpy at the onset of two-phase flow, which is evaluated at the inlet pressure assuming negligible pressure drop in the single-phase region. I_{in} is the coolant enthalpy at the inlet of the micro-channel.

The location of transition to annular flow is determined by the criterion proposed by Taitel and Dukler (1976), wherein the Martinelli parameter $X_{vv,a}$ as defined in equation (13) has a fixed value of 1.6 at the transition point.

$$X_{vv,a} = 1.6 = \left(\frac{\mu_f}{\mu_g} \frac{1-x}{x} \frac{v_f}{v_g} \right)^{0.5} \quad (13)$$

The above relation yields a vapor quality at the onset of annular flow, of about 0.006-0.0064 depending on the fluid properties for the particular analysis.

Two-phase pressure drop

The pressure drop in the two-phase region of the micro-channel can be expressed as the sum of accelerational and the frictional components. The two-phase pressure drop is computed directly, using the correlation provided by Qu and Mudawar (2003a). The Qu and Mudawar (2003a) correlation is based on the combination of laminar liquid and laminar vapor flow assumption (both Re_f and Re_g being less than 2,000) and accounts for the channel size and coolant mass velocity by incorporating channel hydraulic diameter and mass velocity terms in the Martinelli-Chisholm constant C . The pressure drop is given as:

$$\Delta P_{tp} = \Delta P_{tp,f} + \Delta P_{tp,a} \quad (14)$$

The frictional component of the pressure drop $\Delta P_{tp,f}$ is given as:

$$\Delta P_{tp,f} = \frac{L_{tp}}{x_{e,out}} \int_0^{x_{e,out}} \frac{2f_f G^2 (1-x_e)^2 v_f}{D_h} \phi_f^2 dx_e \quad (15)$$

where

$$\phi_f^2 = 1 + \frac{C}{X_{vv}} + \frac{1}{X_{vv}} \quad (16)$$

$$C = 21[1 - \exp(-0.319 \times 10^3 D_h)](0.00418G + 0.0613) \quad (17)$$

$$X_{vv} = \left(\frac{\mu_f}{\mu_g} \right)^{0.5} \left(\frac{1-x_e}{x_e} \right)^{0.5} \left(\frac{v_f}{v_g} \right)^{0.5} \quad (18)$$

The acceleration component of the pressure drop $\Delta P_{tp,a}$ is given as:

$$\Delta P_{tp,a} = G^2 v_f \left[\frac{x^2}{\epsilon_{out}} \left(\frac{v_g}{v_f} \right) + \frac{(1-x_{e,out})^2}{1-\epsilon_{out}} - 1 \right] \quad (19)$$

where

$$\varepsilon_{\text{out}} = \frac{1}{1 + \left(\frac{1-x_{e,\text{out}}}{x_{e,\text{out}}}\right) \left(\frac{v_l}{v_g}\right)^{2/3}} \quad (20)$$

The local pressures are determined by linear interpolation.

Determination of the two-phase heat transfer coefficient

Previous experimental and flow visualization studies by Zhang *et al.* (2000), Jiang *et al.* (2001), etc. have revealed the fact that forced convection boiling is dominant in water cooled micro-channels under high heat flux conditions. Forced convection boiling region is normally associated with annular flow patterns, wherein the heat is transferred mainly by single-phase convection through the annular liquid film. Mukherjee and Mudawar (2003), in their recent study have pointed out that the bubble departure diameters for water are one or two orders greater as compared to those for fluorochemical refrigerants. As a result of this, the vapor bubbles in water quickly engulf the entire channel cross-section triggering off a quick transition to annular flow.

The heat transfer coefficient in the region of annular flow is mainly dependent on the mass velocity of the coolant and vapor quality. In general, the two-phase heat transfer coefficient in water cooled micro-channels increases with increasing G for a given vapor quality and decreases with increasing vapor quality for a fixed G . The trend of decreasing heat transfer coefficient with quality has been observed in many recent experimental studies, such as those carried out by Wambsganss *et al.* (1993), Qu and Mudawar (2003c), Warriar *et al.* (2002), Kew and Cornwell (1997) and Ravigururajan (1998). Warriar *et al.* (2002) have explained this trend by local dry out beneath the vapor bubbles. On the other hand, Qu and Mudawar (2003b) have attributed the above trend to the dominant droplet deposition into the annular liquid film, which increases the liquid film thickness in the stream-wise direction.

Many correlations have been proposed for the determination of the two-phase heat transfer coefficients in mini, micro and macro-channels. Qu and Mudawar (2003c) have studied various correlations for both macro- and micro-channels and have compared the results with their experimental work. It is found that most of the correlations do not capture the trend of decreasing heat transfer coefficient with increasing vapor quality in a water cooled micro-channel. Only the correlation provided by Warriar *et al.* (2002), yields the two-phase heat transfer coefficient with minimum error and with the right trend of decreasing h_{tp} with increasing vapor quality. Hence the correlation developed by Warriar *et al.* (2002) is used in the present analysis and the correlation is given as:

$$\frac{h_{\text{tp}}}{h_{\text{sp}}} = 1 + 6.0\text{Bo}^{\frac{1}{16}} + f(\text{Bo})(x)^{0.65} \quad (21)$$

valid for the following range of parameters:

$$0.03 \leq x \leq 0.55, \quad \text{and} \quad 0.00027 \leq \text{Bo} \leq 0.00089$$

where

$$f(\text{Bo}) = -5.3(1 - 855 \text{Bo}) \quad (22)$$

h_{sp} is the single-phase heat transfer coefficient given by:

$$h_{sp} = Nu_4 \frac{k_f}{D_h} \quad (23)$$

and Nu_4 is the laminar single-phase fully developed Nusselt number, for four sided heating as given by Shah and London (1978):

$$Nu_4 = 8.235(1 - 2.042\alpha^{-1} + 3.085\alpha^{-2} - 2.477\alpha^{-3} + 1.058\alpha^{-4} - 0.186\alpha^{-5}) \quad (24)$$

The Boiling number based on the mean heat flux along the heated perimeter is given as:

$$Bo = \frac{qW}{N(w_c + 2H_c)GI_{fg}} \quad (25)$$

Assuming uniform flux at the base, the local vapor quality is determined by heat balance as:

$$x = \frac{I_{tp} - I_L}{I_{fg}} \quad (26)$$

where the enthalpy of the two-phase fluid I_{tp} at any point in the channel is given by the relation:

$$I_{tp} = I_{IN} + \frac{Q}{\dot{m}A} \quad (27)$$

where I_{IN} is the enthalpy of the inlet fluid and Q is the total heat added up to the point considered. I_L is determined at the inlet pressure assuming negligible pressure drop in the single-phase region. I_{fg} can be determined at the local pressures obtained by linear interpolation.

In order to simulate the actual case of a micro-channel, wherein only three walls are heated, the top wall being typically adiabatic, a correction is made to Warriar *et al.*'s (2002) correlation as suggested by Philips (1990): $h_{tp} = (Nu_3/Nu_4) \times$ Two-phase heat transfer coefficient directly obtained by Warriar *et al.*'s (2002) cocorrelation (equation (21)) where Nu_3 is the laminar single-phase fully developed Nusselt number for three sided heating and is given by Shah and London (1978) as:

$$Nu_3 = 8.235(1 - 1.883\alpha^{-1} + 3.767\alpha^{-2} - 5.814\alpha^{-3} + 5.361\alpha^{-4} - 2.0\alpha^{-5}) \quad (28)$$

Determination of the micro-channel wall temperatures and thermal resistance

Once the local two-phase heat transfer coefficients are accurately determined, suitable boundary conditions are applied and the global stiffness matrix is solved using MATLAB. The complete programme automatically calculates the wall temperature distribution for both the single- and two-phase sections of the micro-channel. The final results of the analysis are presented in the form of thermal resistance of the micro-channel heat exchanger. The thermal resistance in the two-phase section of the micro-channel is obtained from the relation:

$$R_{tp} = \frac{(T_{tp,max} - T_{sat})}{qL_{tp}W} \quad (29)$$

where $T_{tp,max}$ is the maximum wall temperature in the two-phase region of the micro-channel.

Results and discussion

The present finite element formulation and the subsequent analysis for single-phase flow in a micro-channel heat exchanger has been validated against the available results in the literature by Quadir *et al.* (2001). The same method is extended to the two-phase flow region, by determining the two-phase heat transfer coefficient correctly at each location of the micro-channel. The two-phase heat transfer coefficient in the present analysis is determined by the correlation provided by Warriier *et al.* (2002). The results are compared with those of Qu and Mudawar (2003b). The micro-channel dimensions used in the present analysis are given below, which are the same as that in Qu and Mudawar (2003b) in order to facilitate the comparison of the results.

$$W = 1 \text{ cm}$$

$$L = 4.448 \text{ cm}$$

$$w_c = 231 \text{ }\mu\text{m}$$

$$H_c = 712 \text{ }\mu\text{m}$$

$$t = 118 \text{ }\mu\text{m}$$

$$G = 255 \text{ kg/m}^2\text{s}$$

$$N = 21$$

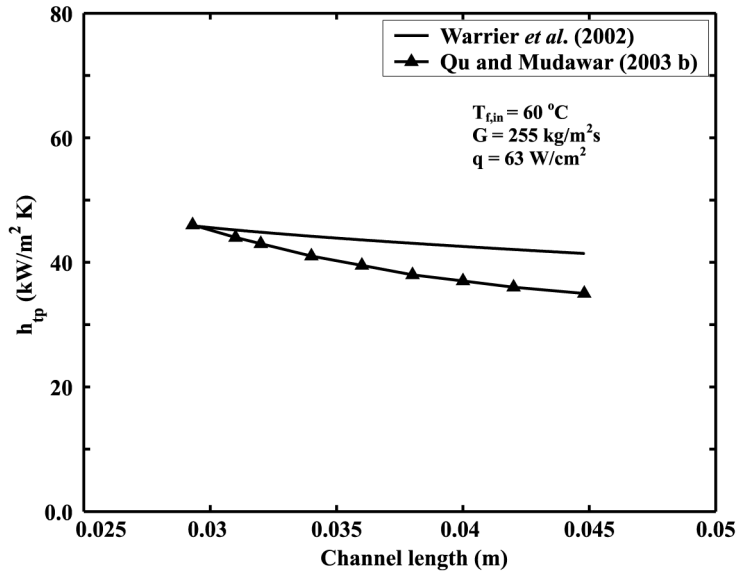
$$\alpha = H_c/w_c = 3.082$$

$$D_h = 3.488 \times 10^{-4} \text{ m}$$

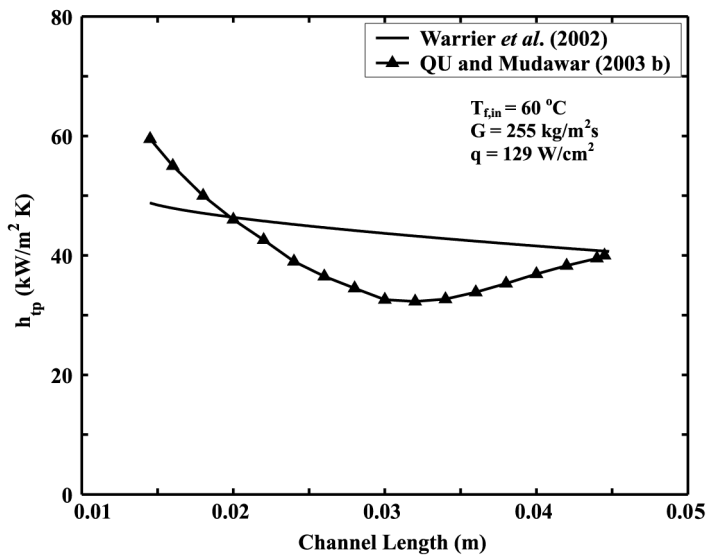
In the present analysis water is considered as the coolant and all the calculations are carried out at a fixed mass flux of $255 \text{ kg/m}^2\text{s}$ while the coolant inlet temperature is fixed at 60°C .

Figure 4 shows the comparison of variation of the two-phase heat transfer coefficient along the channel length, as calculated by Warriier *et al.* (2002) correlation and also through the annular flow model proposed by Qu and Mudawar (2003b), for two different uniform base heat fluxes of 63 and 129 W/cm^2 . At the lower base heat flux (Figure 4(a)), there is a continuous drop in h_{tp} along the channel length shown by both the methods. However, at higher base heat flux (Figure 4(b)), the heat transfer coefficient calculated by Qu and Mudawar initially decreases and then increases. This trend has been attributed to the fact that initially the deposition of the entrained droplets into the liquid film is dominant, due to which the liquid film thickness increases in the stream-wise direction leading to a decrease in the heat transfer coefficient in the stream-wise direction. Further, when the droplet deposition becomes negligible (as discussed later) the film thickness starts decreasing leading to the increasing trend of the heat transfer coefficient. However this trend is not captured by the Warriier *et al.* (2002) correlation, which shows a continuous decrease of h_{tp} in the stream-wise direction. But it should be noted that the average heat transfer coefficients calculated from the two methods agree well with each other with a maximum deviation of 10 percent.

The h_{tp} calculated from Warriier *et al.*'s (2002) correlation is used to determine the annular liquid film thickness δ by the relation $\delta = h_{tp}k_f$ based on the laminar liquid flow assumption as given by Collier and Thome (1994). The film thickness so



(a) Variation of saturated two-phase heat transfer coefficient in the stream-wise direction for $q = 63 \text{ W/cm}^2$



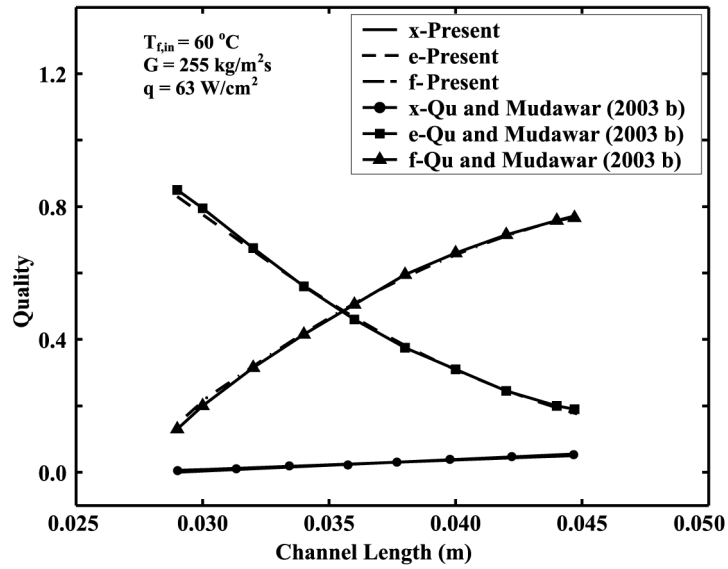
(b) Variation of saturated two-phase heat transfer coefficient in the stream-wise direction for $q = 129 \text{ W/cm}^2$

Figure 4.

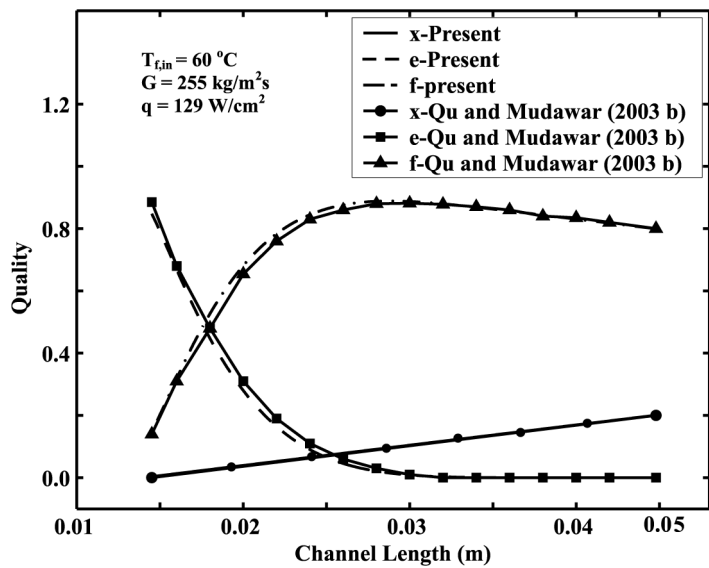
determined is then used to evaluate the liquid film quality f , entrained droplet quality e and vapor quality x along the stream-wise direction, as explained by Qu and Mudawar (2003b). The results are shown in Figure 5 for two different uniform base heat fluxes $q = 63$ and $q = 129 \text{ W/cm}^2$. The reported results of Qu and Mudawar (2003b) for the variation of f , e and x are also plotted in Figure 5. It may be pointed out that Qu and Mudawar (2003b) obtained the value of δ through an iterative procedure, whereas in the present study δ is determined using the h_{tp} obtained from Warriar et al.'s (2002) correlation. It can be seen from Figure 5 that the present results match very well with those of Qu and Mudawar, for both the uniform fluxes. It can be seen that for lower fluxes (Figure 5(a)), the droplet quality continuously decreases while the liquid film quality increases due to dominant droplet deposition from the vapor core into the liquid film. But, at higher fluxes (Figure 5(b)) the droplet quality rapidly decreases at first and becomes negligible indicating that most of the droplets have been already deposited into the liquid film. The liquid film quality increases and then slightly decreases once the droplet quality becomes negligible. The vapor quality monotonically increases in both the cases.

Figure 6 shows the variation of the channel base temperature in the stream-wise direction for single- and two-phase flow for various uniformly distributed fluxes calculated from the finite element analysis. The base temperatures for single-phase flow increase drastically in the stream-wise direction mainly due to the fact the coolant temperature goes on increasing in the stream-wise direction, thus reducing the convection heat transfer driving potential ($T - T_f$). Once the liquid starts boiling the wall temperatures reduce considerably and there is only a small increase in the base temperatures thereafter. The considerable decrease in wall temperatures at the onset of two-phase flow can be attributed to the fact that the heat transfer coefficient for the two-phase flow increases considerably ($\sim 45,000 \text{ W/cm}^2 \text{ K}$) from that for the fully developed laminar single-phase flow ($\sim 10,000 \text{ W/cm}^2 \text{ K}$) for the present micro-channel dimensions. It is also noted from Figure 6 that the base temperature in the two-phase flow region for a given flux is almost uniform. This is due to the fact that the driving potential ($T - T_f$) almost remains constant along the stream-wise direction for the two-phase flow region. It is further noticed that for the present mass flux (G) of $255 \text{ kg/m}^2 \text{ s}$ and coolant inlet temperature (T_{in}) of 60°C , a lower base heat flux viz. 40 W/cm^2 will not result in the boiling of the coolant and therefore, the coolant remains as a single-phase liquid throughout the channel length leading to a continuous increase in the micro-channel base temperature.

One of the main advantages of the present method of analysis using FEM is that the micro-channel performance can be analyzed even for non-uniform base heat fluxes. In order to demonstrate this, a case of non-uniform base heat flux is also considered in the present analysis. For this purpose the micro-channel is divided into 20 equal parts in the stream-wise direction and a non-uniform base heat flux is distributed in these parts as shown in Table I. The flux is distributed linearly in an ascending order along the length of the channel. Figure 7 shows the micro-channel base and coolant temperature variations in the stream-wise direction for the case of non-uniform flux distribution of Table I with $q = 150 \text{ W/cm}^2$. Also for the sake of comparison the base and fluid temperature variations with uniform flux are plotted for the same total base heat flux in the same figure. It can be seen from Figure 7 that the onset of two-phase flow for the proposed non-uniform base heat flux distribution, is delayed as compared to that of



(a) Variation of liquid film quality, liquid droplet quality and vapor quality along the stream-wise direction for $q = 63 \text{ W/cm}^2$



(b) Variation of liquid film quality, liquid droplet quality and vapor quality along the stream-wise direction for $q = 129 \text{ W/cm}^2$

Figure 5.

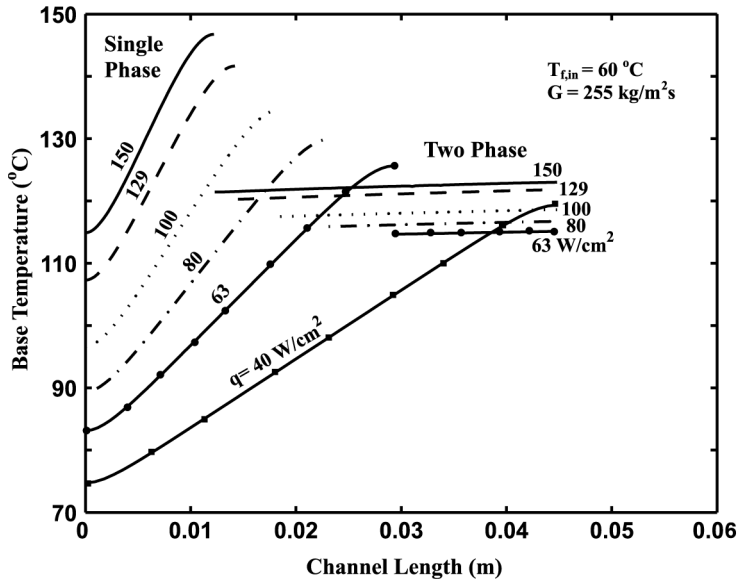


Figure 6. Variation of the micro-channel base temperature in the stream-wise direction for both single - and two-phase flows for uniform base heat fluxes

Non-uniform base heat flux distribution for 20 equal parts (assumed) along the length of the channel, W/cm^2	$0.1q$	$0.2q$	$0.3q$	$0.4q$	$0.5q$	$0.6q$	$0.7q$	$0.8q$	$0.9q$	$1.0q$
Uniform base heat flux distribution, W/cm^2	$1.1q$	$1.2q$	$1.3q$	$1.4q$	$1.5q$	$1.6q$	$1.7q$	$1.8q$	$1.9q$	$2.0q$
	Total base heat flux = $21q$									
	Total base heat flux = $20 \times 1.05q = 21q$									

Table I. Assumed uniform and non-uniform heat flux distribution on the base of the micro-channel

uniform flux due to the fact that lower heat fluxes are distributed in the earlier parts of the channel. The variation of the fluid temperature in the stream-wise direction is also shown for the above-mentioned two cases.

The maximum wall temperatures for the single- and two-phase sections of the micro-channel are separately evaluated by FEM and then the corresponding thermal resistances of the micro-channel sections are calculated. Table II shows the comparison of single- and two-phase thermal resistances of the micro-channel at different uniform fluxes ranging from 40 to 150 W/cm^2 . The two-phase thermal resistance is at least one order less when compared to the single-phase thermal resistance. Also it is interesting to note that the single-phase thermal resistance increases with heat flux while the two-phase thermal resistance decreases with increasing flux. Table III gives the actual pressure drops in the single- and two-phase sections of the micro-channel for different base heat fluxes as well as the corresponding pressure drops per unit length of the micro-channel. It is evident from this table that the pressure drop per unit length for the single-phase flow remains almost constant whereas the two-phase pressure drop per unit length increases considerably with heat flux. An examination of Table III also shows that the advantage of reduced resistance in two-phase flow can be gained only at the cost of increased pressure drop.

Figure 7.
Variation of the micro-channel base temperature and fluid temperature in the stream-wise direction for both uniform and non-uniform base heat fluxes

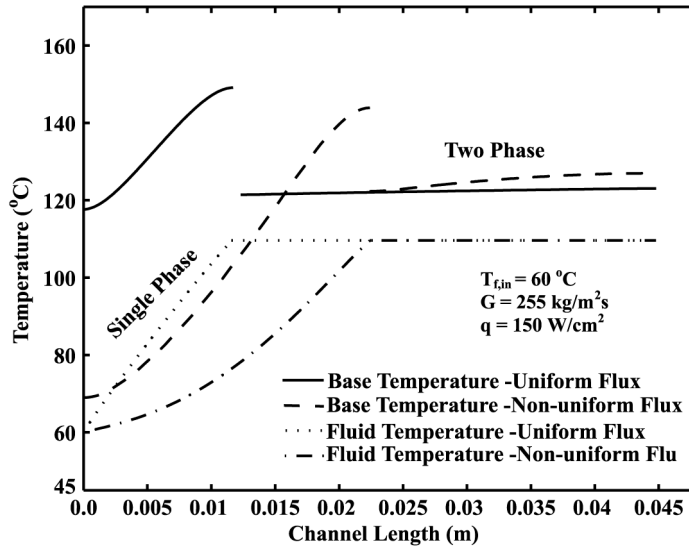


Table II.
Thermal resistance for the micro-channel for different uniform base heat fluxes

Base heat flux (W/cm^2)	63	80	100	129	150
Thermal resistance for the single-phase region of the micro-channel ($^{\circ}\text{C/W}$)	0.355	0.379	0.4058	0.4458	0.474
Thermal resistance for the two-phase region of the micro-channel ($^{\circ}\text{C/W}$)	0.0576	0.0412	0.0344	0.0315	0.0268

Table III.
Pressure drop across the micro-channel for different uniform base heat fluxes

Base heat flux (W/cm^2)	63	80	100	129	150
Pressure drop for the part of the channel experiencing single-phase flow (bar)	0.0055	0.0043	0.0034	0.0027	0.0022
Pressure drop for the part of the channel experiencing two-phase flow (bar)	0.026	0.050	0.079	0.129	0.173
Total pressure drop for the entire channel (bar)	0.0315	0.061	0.082	0.132	0.175
$\Delta P = \Delta P_{\text{sp}} + \Delta P_{\text{tp}}$					
Single-phase pressure drop per unit length (bar/m)	0.189	0.183	0.178	0.175	0.172
Two-phase pressure drop per unit length (bar/m)	1.72	2.30	3.00	4.26	5.38

Conclusions

The FEM is used to analyze two-phase flow in a rectangular cross section micro-channel. Water enters the channel in a sub-cooled state and subsequently boils in the channel. The present methodology is also able to analyze both uniform and non-uniform base heat fluxes. Based on the results of the present analysis the following conclusions can be drawn.

- (1) It can be noted from the analysis that the thermal resistances in two-phase flow are at least one order less when compared to the single-phase thermal resistances.
- (2) The single-phase thermal resistance increases with heat flux while the two-phase thermal resistance decreases with increasing heat flux.
- (3) Two-phase flow yields better wall temperature uniformity in the stream-wise direction.
- (4) The improved thermal resistance in two-phase flow can be achieved only at the cost of increased pressure drop.

References

- Bergles, A.E. and Dorrmer, T. Jr (1969), "Subcooled boiling pressure drop with water at low pressure", *International Journal of Heat and Mass Transfer*, Vol. 12, pp. 459-70.
- Collier, J.G. and Thome, J.R. (1994), *Convective Boiling and Condensation*, 3rd ed., Oxford University Press, Oxford press.
- Jiang, L., Wong, M. and Zohar, Y. (2001), "Forced convection boiling in a microchannel heat sink", *J. Microelectromech. Syst.*, Vol. 10 No. 1, pp. 1080-7.
- Kew, P.A. and Cornwell, K. (1997), "Correlations for the prediction of boiling heat transfer in small-diameter channels", *Appl. Therm. Eng.*, Vol. 17, pp. 705-15.
- Kim, S.J. and Kim, D. (1999), "Forced convection in microstructures for electronic equipment cooling", *ASME J. Heat Transfer*, Vol. 121, pp. 639-45.
- Lewis, R.W., Morgan, K., Thoma, H.R. and Seetharamu, K.N. (1996), *The Finite Element Method in Heat Transfer Analysis*, Wiley and Sons, New York, NY.
- Mukherjee, S. and Mudawar, I. (2003), "Pumpless loop for narrow channel and micro-channel boiling", *J. Electron. Package*, Vol. 125, pp. 431-41.
- Peng, X.F. and Peterson, G.P. (1996), "Convective heat transfer and flow friction for water flow in microchannel structures", *International Journal of Heat and Mass Transfer*, Vol. 39, pp. 2599-608.
- Philips, R.J. (1990), "Microchannel heat sinks", in Bar-Cohen, A. and Kraus, A.D. (Eds), *Advances in Thermal Modeling of Electronic Components and Systems*, ASME, New York, NY, pp. 109-84.
- Qu, W. and Mudawar, I. (2002), "Prediction and measurement of incipient boiling heat flux in micro-channel heat sinks", *International Journal of Heat and Mass Transfer*, Vol. 45 No. 19, pp. 3933-45.
- Qu, W. and Mudawar, I. (2003a), "Measurement and prediction of pressure drop in two-phase micro-channel heat sinks", *International Journal of Heat and Mass Transfer*, Vol. 46, pp. 2738-53.
- Qu, W. and Mudawar, I. (2003b), "Flow boiling heat transfer in two-phase micro-channel heat sinks – II. Annular two-phase flow model", *International Journal of Heat and Mass Transfer*, Vol. 46, pp. 2773-84.
- Qu, W. and Mudawar, I. (2003c), "Flow boiling heat transfer in two-phase micro-channel heat sinks – I. Experimental investigation and assessment of correlation methods", *International Journal of Heat and Mass Transfer*, Vol. 46, pp. 2755-71.
- Qu, W. and Mudawar, I. (2004), "Measurement and correlation of critical heat flux in two phase micro-channel heat sinks", *International Journal of Heat and Mass Transfer*, Vol. 47, pp. 2045-59.

Quadir, G.A., Anvar, M. and Seetharamu, K.N. (2001), "Analysis of microchannel heat exchangers using FEM", *International Journal of Numerical Methods for Heat and Fluid Flow*, Vol. 11 No. 1, pp. 59-75.

Ravigururajan, T.S. (1998), "Impact of channel geometry on two phase flow heat transfer characteristics of refrigerants in microchannel heat exchangers", *J. Heat Transfer*, Vol. 120, pp. 485-91.

Segerlind, L.J. (1984), *Applied Finite Element Methods*, Wiley, New York, NY.

Shah, R.K. and London, A.L. (1978), *Laminar Flow Forced Convection in Ducts: A Sourcebook for Compact Heat Exchanger Analysis Data*, Supl. 1, Academic Press, New York, NY.

Taitel, Y. and Dukler, A.E. (1976), "A model for predicting flow regime transition in horizontal and near horizontal gas-liquid flow", *AIChE Journal*, Vol. 22, pp. 47-55.

Toh, K.C., Chen, X.Y. and Chai, J.C. (2002), "Numerical computation of fluid flow and heat transfer in micro-channels", *International Journal of Heat and Mass Transfer*, Vol. 45, pp. 5133-41.

Tuckerman, D.B. and Pease, R.F.W. (1981), "High performance heat sink for VLSI", *IEEE Electron Device Letters*, Vol. EDL-2 No. 4, pp. 126-9.

Wambsganss, M.W., France, D.M., Jendrzeczyk, J.A. and Tran, T.N. (1993), "Boiling heat transfer in a horizontal small diameter tube", *Journal of Heat Transfer*, Vol. 115, pp. 963-72.

Warrier, G.R., Dhir, V.K. and Momoda, L.A. (2002), "Heat transfer and pressure drop in narrow rectangular channels", *Exp. Therm. Fluid Sci.*, Vol. 26, pp. 53-64.

Zhang, L., Koo, J.M., Jiang, L., Bannered, S.S., Ashegi, M., Goodson, K.E., Santiago, J.G. and Kenny, T.W. (2000), "Measurement and modeling of two-phase flow in microchannels with nearly-constant heat flux boundary conditions", in Lee, A., *et al.* (Eds), *Micro-Electro-Mechanical Systems MEMS – ASME*, MEMS-Vol. 2, ASME, Orlando, FL, pp. 129-35.

Zhimin, W. and Fah, C.K. (1997), "The optimum thermal design of microchannel heat sinks", *IEEE/CPMT Electronic Packaging Technology Conference*, pp. 123-9.

Further reading

Bowers, M.B. and Mudawar, I. (1994), "High flux boiling in low flow rate, low pressure drop mini-channel and micro-channel heat sinks", *International Journal of Heat and Mass Transfer*, Vol. 37 No. 2, pp. 321-32.